Explosive Vaporization of Metallic Sodium Microparticles by CW Resonant Laser Radiation

S. N. Atutov,[1,*] W. Baldini,[1] V. Biancalana,[2] R. Calabrese,[1] V. Guidi,[1,†] B. Mai,[1] E. Mariotti,[2] G. Mazzocca,[1] L. Moi,[2] S. P. Pod'yachev,[1,*] and L. Tomassetti[1]

[1]*Dipartimento di Fisica dell'Università, INFN, Sezione di Ferrara, I-44100 Ferrara, Italy*
[2]*INFM, Unità di Siena, Dipartimento di Fisica dell'Università, I-53100 Siena, Italy*
(Received 2 May 2001; published 1 November 2001)

Explosive vaporization of metallic Na microparticles stimulated by resonant cw laser radiation has been observed in a glass cell. Vaporization occurs at low laser-power density. The effect consists in the generation of optically thick and sharply localized Na vapor clouds propagating in the cell against the laser beam. The effect is explained by laser excitation of Na atoms, which collide onto the surface of the microparticles and transfer their internal energy. This causes other atoms to be vaporized and to continue the avalanche process.

PACS numbers: 52.35.Mw, 52.38.Mf, 32.80.–t

Generation and vaporization of metallic alkali microparticles within an optical cell operating in heat-pipe-oven (HPO) regime are relatively complex processes to be studied in detail. Indeed, HPO operation is based on dynamical equilibrium in a heterogeneous phase and known to depend on many parameters [1]. Yet, these processes may be helpful in understanding the ablation of metallic particles or the damage of metallic surfaces by light.

Because of its relatively simple atomic structure and ease of implementation in a cell, sodium is definitely a good candidate for studying the generation and vaporization of metallic microparticles. Under certain conditions, metallic sodium microparticles (MSM) can be formed at the vapor-to-noble-gas interface where a supersaturated vapor is obtained and abruptly condenses due to a negative temperature gradient. As an example, Granqvist and Buhrman [2] produced MSM by simply evaporating a metal in the presence of a buffer gas. MSM formation has also been obtained by breaking the dynamic equilibrium at the vapor-gas interface. For example, huge production of potassium microparticles in HPO has been observed as a consequence of strong laser excitation of K_2 molecules [3].

We have observed explosive vaporization of metallic sodium microparticles by resonant cw dye-laser radiation. MSM vaporization generates an optically thick, bright, and sharply localized Na vapor cloud which moves opposite to the direction of propagation of the laser beam. Then other clouds are formed to generate a periodic sequence propagating in the cell. The clouds exhibit "solitonlike" behavior; i.e., there is no change is shape, size, brightness, and velocity during propagation over a distance that can be very long with respect to the cloud size.

This intriguing and unexpected effect occurs in the presence of high-pressure buffer gas within an optical cell operating in a HPO regime and only when the frequency of the laser radiation is sharply tuned to the D_1 and D_2 atomic absorption lines of Na atoms. No cloud generation is found when the laser beam passes through the MSM fog but not through the vapor in the hot part of the cell, or when the laser radiation is strongly focused. These facts exclude that the observed effect can be explained in terms of the standard knowledge on laser ablation due to the low level of power density involved (in the W/cm^2 range) or by coherent phenomena on MSM such as surface plasmons [4]. Rather, it involves direct collision of excited atoms onto MSM with transfer of the internal energy from the atoms to the particle. Evidence of solitonlike Na vapor propagation—though under a completely different regime—has been reported by Werij and Woerdman in a capillary [5].

The experimental apparatus is sketched in Fig. 1. It consists of a glass HPO cell illuminated by a dye laser. The cell is a Pyrex glass tube 20 mm in diameter and 500 mm in length filled by Ar as a buffer gas up to 900 mbar. A piece of Na metal is located close to one of the cell ends where an electrical heater allows the temperature to reach about 530 K. Such a temperature is high enough to produce an optically thick Na vapor localized within the hottest part of the cell. The laser beam is aligned along the cell axis and used for illuminating the Na vapor. Its diameter is smaller than the cell diameter and variable from 1 to 8 mm. The laser power used in the experiment ranges from 100 to 800 mW. The frequency of the laser radiation can be tuned to either the D_1 or the D_2 Na atomic absorption line.

The propagation of the Na vapor cloud along the cell axis is recorded by fluorescence detection at two locations spaced by 120 mm along the cell axis. Two photodiodes (pd1 and pd2) provide determination of the fluorescence spot size with a spatial resolution of 200 μm. The photodiodes are also used to determine the mean velocity of the propagating Na cloud. Moreover, the vapor density distribution is measured, with a 200 μm spatial resolution, by a probe beam streamed off the main laser beam and directed transversely to the cell. The probe beam is attenuated, in order to avoid saturation in the optical transition. A third photodiode (pd3) is placed 5 m far from the cell, where the intensity of fluorescence is negligible as compared to the probe-beam intensity.

Soon after the temperature has reached 530 K, MSM appear and spread fairly uniformly along the cold part of
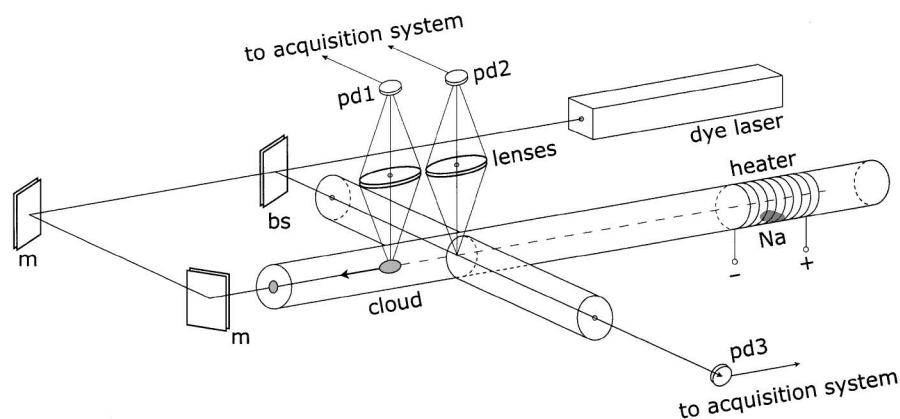
FIG. 1. Sketch of the experimental apparatus. The arrow indicates the propagation direction of the vapor clouds. Na = metallic piece of sodium. pd1, pd2, pd3 = photodiodes; m = mirrors; bs = beam splitter.

the cell. The MSM are formed on the border between the cold and hot zones due to Na vapor condensation in the presence of the buffer gas. The concentration of MSM has been found to vary in an uncontrollable way at each run of measurements. This leads to qualitatively equivalent results for all the runs but the values of experimental parameters may jitter from run to run.

In our experimental conditions, the particles look like structureless bright points when observed through a microscope. Once the oven has been switched off, the dust falls on the cell bottom in several hours. These are indications that the size of MSM is smaller than the laser wavelength. When operating with the dye laser not tuned to the D absorption lines of Na, the dust of particles scatters the laser photons and no vaporization is observed. In this case the laser beam attenuation is negligible—an evidence that direct laser-to-MSM interaction does not play any significant role.

When the laser radiation is tuned on resonance to D_1 or D_2 lines of Na, the laser beam is completely absorbed within the hot part of the cell. Here, a bright and compact Na vapor cloud is formed on the border between the hot and cold parts of the cell. Then the cloud starts moving against the laser beam at fairly constant velocity. The movement of the cloud proceeds until the propagating front encounters a portion of the cell with lower density of MSM. Here the cloud becomes very weak and disappears with a decay time of about 10 ms. Then, another cloud is formed on the border between the hot and cold parts and the process starts again. Interruption of the laser beam for a time interval much shorter than 10 ms gives no effect to the cloud movement, while interruption for a time longer than 10 ms leads to an abrupt decay of the cloud. Typical MSM density for the avalanche process to be sustained is about 10^6 cm^{-3} as measured by a microscope equipped with a CCD camera. Excitation by resonant laser radiation alters the dynamical equilibrium of sodium among metallic clusters and the vapor phase: a time of 10 ms is therefore the characteristic time to vary such equilibrium. Other effects such as the diffusion of Na vapor out of the

laser beam should not be called forward when operating at wide laser diameter and high pressure. In fact, the time taken by Na atoms to escape the laser-beam region, $T = (r^2/4D)^{1/2}$, is estimated to be about 400 ms, i.e., too long to explain the process, $r = 4$ mm being the laser-beam radius and $D = 0.25$ cm^2/s the diffusion coefficient at 900 mbar [6].

When MSM are nearly homogeneously distributed within the whole cell, a cloud moves in the cell and sticks onto the entrance window for the laser. Here the cloud keeps staying at the window for several minutes and abruptly disappears in a time of the order of 10 ms. Then, a new cloud is generated. In this case, cloud propagation has been observed to continue for about half an hour, then it falls off due to reflection of the laser beam onto the metallic layer deposited at the entrance window through bombardment by Na clouds. The deposition has the same size and form as the laser beam and can be cleaned up by heating the cell window. This kind of deposition has never been observed without generation and propagation of Na clouds.

A typical fluorescence signal of the photodiodes is shown in Fig. 2 together with the absorption signal of the probe beam. This latter indicates that the distribution of Na vapor inside the cloud is not symmetric, as the front of the cloud is steeper than the back. The profile of the fluorescence peak is narrower than the vapor distribution because laser radiation is completely absorbed just at the beginning of the optically thick cloud. The inset shows the fluorescence signals from the pd1 and pd2 photodiodes due to the transit of a train of vapor clouds. In this case, the cloud production rate is about 1 Hz, the cloud velocity $v_c \cong 500$ mm/s, and a cloud length $L_c \cong 18$ mm.

The dependence of the cloud velocity on the laser power and buffer gas pressure are shown in Figs. 3 and 4, respectively. An increase in the laser power causes an increase in velocity until a saturation level is reached. At low buffer-gas pressure, a velocity as high as 2 m/s has been measured. A common feature of the curves is the appearance of a threshold.
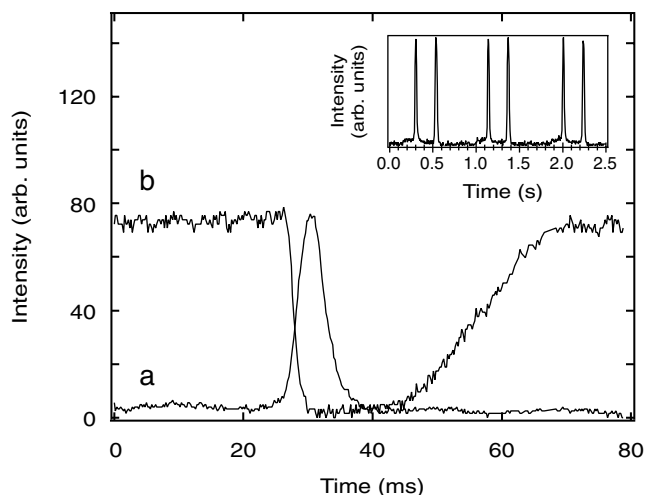
FIG. 2. (*a*) Na-cloud fluorescence signal (photodetector pd1) and (*b*) transmitted probe-beam signal (photodector pd3) as a function of time. The signals are taken during the passage of the cloud through the cell at 800 mW laser power, 900 mbar buffer-gas pressure, and 8 mm laser beam diameter. The inset shows a typical fluorescence signal taken at pd1 and pd2 in which is visible the periodic structure of the propagating cloud. The distance from pd1 to pd2 is 120 mm. The pedestal in the signal recorded by pd2 is due to stray light originated at the cell wall deformed to host the transverse tube (see Fig. 1).

By using the probe beam, it has been checked that the cloud has a well defined form and that vapor concentration out of the cloud is negligible, probably due to condensation of vapor back into the MSM. A sufficiently wide diameter of the laser beam and the presence of a buffer gas are important to prevent a large loss of atoms due to diffusion out from the laser beam and to keep a sufficiently dense vapor for the process to be sustained. Resonance-radiation trapping also feeds cloud generation and propagation.

No cloud generation is found when the Na heater is switched off, or the laser beam passes through the dust of MSM but not through the hot part of the cell, or when the laser radiation is strongly focused, for example, down to a spot of 100 μm in diameter within the cold area of the cell. These facts exclude vaporization by direct heating of the surface of MSM by light.
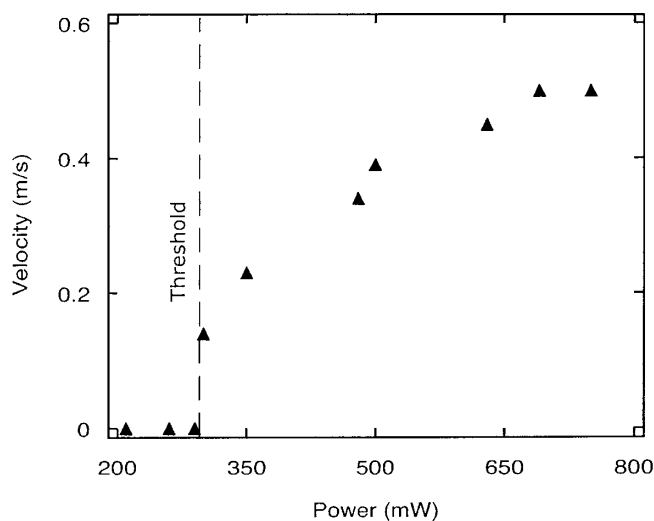
According to the features of the effect, it is clear that atomic density is a key parameter to be considered. The sodium saturated vapor density at 525 K is $n \cong 10^{14}$ cm^{-3} [7]. In the experiment the vapor is not at thermodynamic equilibrium with solid Na and we therefore expect a smaller value; n can be evaluated by considering the absorption length of the laser light. The width of the atomic absorption line is pressure broadened by the buffer gas and is larger than both Doppler width and hyperfine splitting of the *D* lines [8]. In this case, the following expressions hold true for light-absorption cross section, σ:

$$\sigma = \frac{\sigma_0}{1 + I/I_s}, \qquad \sigma_0 = \frac{\lambda^2}{4\pi}\frac{A}{\Gamma}\frac{g_p}{g_s}, \qquad (1)$$

where σ_0 is the cross section for nonsaturated absorption, I is the light intensity, I_s is the saturation intensity, λ is the laser wavelength, A is the spontaneous decay rate, Γ is the pressure-broadened width of absorption line, and g_s, g_p are the statistic weights for the ground and excited states of the atomic transition. In the experiment, we have operated with a moderate light intensity (~ 1.0 W/cm^2), i.e., at a level essentially lower than the saturation intensity. In fact, one calculates $\sigma \sim 5.4 \times 10^{-13}$ cm^2 for the D_2 Na line ($I_s \sim 26$ W/cm^2) at 900 mbar buffer-gas pressure. The length of light absorption has been measured to be less than 4 mm; therefore, by taking into account the value of cross section, one determines the effective atomic density of the clouds to be about 10^{13} cm^{-3}. Such an atomic density is high enough to trigger many different processes involving energy transfer, energy pooling, and ionization collisions [9]. All these processes can easily be detected

FIG. 3. Dependence of Na-cloud velocity v_c vs laser power at 900 mbar buffer-gas pressure, 8 mm laser beam diameter. Clearly visible is a threshold for cloud propagation.
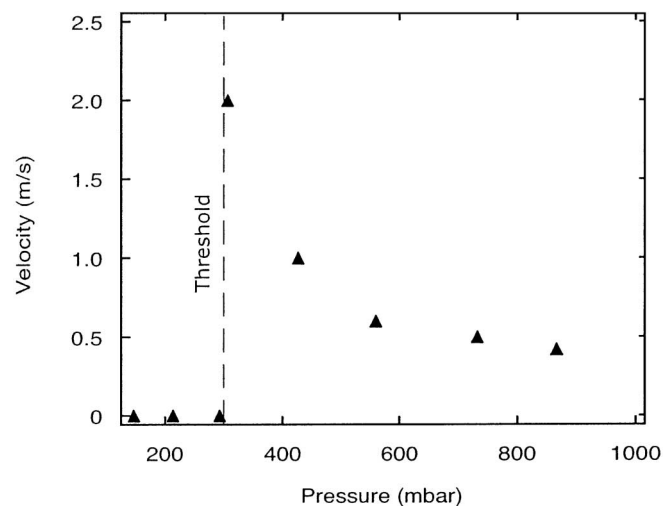
FIG. 4. Dependence of No-cloud velocity vs buffer gas pressure at 800 mW laser power, 8 mm laser beam diameter. When the pressure of the buffer gas is sufficiently high to prevent atomic diffusion, cloud propagation begins.

through the fluorescence spectral analysis due to the appearance of atomic lines different from the fundamental D of sodium. No such signals have been detected in the present experiment so that they can be neglected with their related processes.

At first sight, one might expect that the process driving vapor-cloud generation and propagation is pure thermal vaporization of the MSM due to not identified heating processes, resulting in a temperature increase of the buffer gas. We show that this mechanism is not possible in any case, by estimating the largest possible temperature increase δT in the buffer gas:

$$\delta T \leq \alpha W_0 / \pi r^2 c_p v \,, \qquad (2)$$

where c_p is specific heat capacity of the buffer gas, v is the cloud velocity, and α is the fraction of laser power being absorbed for vaporization of atoms [thus $(1 - \alpha)$ feeds fluorescence]. For typical experimental conditions, such as $r = 4$ mm, $W_0 = 0.5$ W, $v = 0.4$ m/s, and at 900 mbar pressure, one obtains $\delta T \approx 30\alpha$ K. It is clear that even when the whole power would heat the gas ($\alpha = 1$), the temperature increase should be no greater than 30 K. This level is, however, not high enough to allow a concentration of about 10^{13} cm^{-3} through vaporization of the MSM. As a confirmation, heating of a portion of the cell by an extra heater has been imparted. It has been observed that detectable vaporization needs a temperature 200 K higher than room temperature—a level much higher than the calculated 30 K increase.

On the basis of the experimental findings, one is led to interpret the evaporation of Na particles in terms of collisions of excited thermalized atoms (carrying about 2.1 eV energy per atom) with metallic particles. Energy is transferred locally, thus heating a small area on the MSM surface. Then, it results in bond breaking (1.13 eV) and fast vaporization of Na atoms. In the range of pressure we have operated, vaporized atoms do not diffuse too rapidly from the surface of MSM due to the confinement exerted by the buffer gas. If the laser power exceeds the threshold level, then the bombardment rate of excited atoms onto MSM becomes high enough to overcome the rate of losses. In this way, an avalanche of collisions commences leading to vaporization of the MSM. The avalanche process is determined by the vapor in the neighborhood of MSM. Because of the size of MSM (about 1 μm), much larger than the atom size, the vaporized atoms have a 50% probability to collide back onto the MSM surface. Under the regime of deep saturation for optical transition, about half of the atoms are excited due to interaction with the laser. Thus, about 25% of all vaporized atoms can vaporize other atoms by impact onto the MSM surface.

Other than MSM density, the key parameters of the experiment are MSM size, morphology of MSM, and binding energy of surface atoms.

The process of formation and propagation of Na vapor cloud can be explained as follows. At the beginning of the process, laser radiation passes through the cold part of the cell and encounters a relatively high density of Na on the border between the hot and cold parts of the cell. Here light is absorbed leading to a rapid vaporization of neighboring MSM, thus increasing vapor concentration. Part of Na atoms diffuse opposite to the direction of the laser beam towards the cold part of the cell; therefore the location where the laser radiation is mostly absorbed moves to the same direction. This front of vapor impinges onto other metallic Na particles and yields additional Na vapor. Finally, a "wave" of vapor is being generated and runs opposite to the laser beam.

Other evaporation mechanisms based on atomic desorption stimulated by laser-induced surface-plasmon excitation acting on the surface of MSM must be excluded. In our case, in fact, the desorption rate as a function of the photon energy does not show a sharp resonance as indeed was reported by Hoheisel *et al.* for laser-induced surface-plasmon excitation [4]. Moreover, in that case no threshold effect was observed as confirmed also by Balzer *et al.* [10].

The described effect of particle vaporization may be helpful in understanding the ablation of metallic particles or the damage of metallic surface at relatively low laser power density.

---

*Permanent address: Institute of Automation and Electrometry, Novosibirsk 90, Russia.
†Corresponding author.
Present address: Department of Physics, University of Ferrara, Via Paradiso 12, 44100 Italy.
Email address: guidi@fe.infn.it

[1] C. R. Viadal and J. Cooper, J. Appl. Phys. **40**, 3370 (1969).
[2] C. G. Granqvist and R. A. Buhrman, J. Appl. Phys. **47**, 2200 (1976).
[3] M. Allegrini, P. Bicchi, D. Dattrino, and L. Moi, Opt. Commun. **49**, 39 (1984).
[4] W. Hoheisel, K. Jungmann, M. Vollmer, R. Weidenauer, and F. Trager, Phys. Rev. Lett. **60**, 1649 (1988).
[5] H. G. C. Werij and J. P. Woerdman, Phys. Rep. **169**, 204 (1988).
[6] N. S. Atutov, I. E. Ermolaev, and A. M. Schalagin, Sov. Phys. JETP **63**, 1149 (1986).
[7] A. N. Nesmeyanov, *Vapor Pressure of the Chemical Elements* (Elsevier, London, 1963).
[8] E. L. Lewis, Phys. Rep. **58**, 1–71 (1980).
[9] See, for example, A. Kopystynska and L. Moi, Phys. Rep. **92**, 135 (1982).
[10] F. Balzer, M. Hartmann, M. Renger, and H.-G. Rubahn, Z. Phys. D **28**, 321 (1993).